Neuroscience 274 (2014) 369–382

CORTICOSTERONE AFFECTS THE DIFFERENTIATION OF A NEURONAL CEREBRAL CORTEX-DERIVED CELL LINE THROUGH MODULATION OF THE NICOTINIC ACETYLCHOLINE RECEPTOR

C. J. BAIER,[a,b*†] D. L. FRANCO,[a†] C. E. GALLEGOS,[c] L. A. MONGIAT,[d] L. DIONISIO,[e] C. BOUZAT,[e] P. CAVIEDES[f‡] AND F. J. BARRANTES[a*]

[a] *Laboratory of Molecular Neurobiology, Institute of Biomedical Research (BIOMED)-UCA-CONICET, Faculty of Medical Sciences, Pontifical Catholic University of Argentina, and CONICET, Buenos Aires, Argentina*

[b] *Instituto de Investigaciones Bioquímicas de Bahía Blanca, Argentina*

[c] *Laboratorio de Toxicología, Departamento de Biología, Bioquímica y Farmacia, Universidad Nacional del Sur, Bahía Blanca, Argentina*

[d] *Laboratorio de Plasticidad Neuronal, Fundación Instituto Leloir-CONICET, Buenos Aires, Argentina*

[e] *Laboratorio de Neurofisiología y Farmacología Molecular, Instituto de Investigaciones Bioquímicas de Bahía Blanca, B8000FWB Bahía Blanca, Argentina*

[f] *Program of Molecular and Clinical Pharmacology, ICBM, Faculty of Medicine, University of Chile, Santiago, Chile*

Abstract—Chronic exposure to stress hormones has an impact on brain structures relevant to cognition. Nicotinic acetylcholine receptors (AChRs) are involved in numerous cognitive processes including learning and memory formation. In order to better understand the molecular mechanisms of chronic stress-triggered mental disease, the effect of corticosterone (CORT) on the biology of AChRs was studied in the neuronal cell line CNh. We found that chronic treatment with CORT reduced the expression levels of the α7-type neuronal AChR and, to a lesser extent, of α4-AChR. CORT also delayed the acquisition of the mature cell phenotype in CNh cells. Chronic nicotine treatment affected the differentiation of CNh cells and exerted a synergistic effect with CORT, suggesting that AChR could participate in signaling pathways that control the cell cycle. Overexpression of α7-AChR-GFP abolished the CORT effects on the cell cycle and the specific α7-AChR inhibitor, methyllycaconitine, mimicked the proliferative action exerted by CORT. Whole-cell voltage-clamp recordings showed a significant decrease in nicotine-evoked currents in CORT-treated cells. Taken together, these observations indicate that AChRs, and the α7-AChR in particular, could act as modulators of the differentiation of CNh cells and that CORT could impair the acquisition of a mature phenotype by affecting the function of this AChR subtype.

Key words: nicotine, ion channel, glucocorticoids, cell cycle, stress.

INTRODUCTION

The nicotinic acetylcholine receptor (AChR) is a heterogeneous family of ion channels distributed in the central and peripheral nervous systems and non-neural tissues. Channel opening is controlled by the endogenous neurotransmitter acetylcholine and by ligands such as nicotine. The AChR is made up of different subtypes of homo- or hetero-pentameric oligomers distributed throughout different regions of the CNS. Some are located presynaptically, where they modulate the release of other neurotransmitters, such as dopamine; others are found in cell bodies and dendrites, where they exert postsynaptic effects (Gotti et al., 2006). The two main subtypes of AChR in the CNS are α_7 and $\alpha4\beta2$, which are primarily expressed in brain regions that are tightly linked to the neuropathology of Alzheimer's disease. They have also been associated with the pathogenesis of dementia (Oddo and LaFerla, 2006).

Chronic exposure to stress hormones has an impact on brain structures involved in cognition and mental health (Lupien et al., 2009). There is consensus that accelerated age-related cognitive decline is related to an impaired response of the hypothalamic–pituitary–adrenal (HPA) axis (Pardon and Rattray, 2008). In turn, the deregulation of this axis has been related to neurodegenerative diseases, including Alzheimer's disease (Green et al., 2006). In humans, it has been reported that susceptibility to stress increases the risk of developing Alzheimer's disease (Pardon and Rattray, 2008). Under normal conditions, glucocorticoids (GCs) are necessary for adequate brain function, but in excess they modify neurotransmission systems and the transcriptional machinery. In excess amounts they also permanently alter the HPA axis, other

*Corresponding authors. Address: Laboratory of Molecular Neurobiology, Faculty of Medical Sciences, Biomedical Research Institute (BIOMED) UCA–CONICET, Avenida Alicia Moreau de Justo 1600, C1107AFF Buenos Aires, Argentina. Tel: +54-114349-0200x2116.
E-mail addresses: pcaviede@med.uchile.cl (P. Caviedes), rtfjb1@yahoo.com (F. J. Barrantes).

† These two authors contributed equally to this work.

‡ Correspondence regarding the use of the CNh cell line.

Abbreviations: AChR, nicotinic acetylcholine receptor; ANOVA, analysis of variance; CORT, corticosterone; EGTA, ethylene glycol tetraacetic acid; GCs, glucocorticoids; HEPES, 4-(2-hydroxyethyl) piperazine-1-ethanesulfonic acid; HPA, hypothalamic–pituitary–adrenal; MLA, methyllycaconitine; PBS, phosphate-buffered saline; PI, propidium iodide; RT, room temperature.

http://dx.doi.org/10.1016/j.neuroscience.2014.05.049
0306-4522/

endocrine systems and behavior and brain morphology (Lesage et al., 2001; Pardon and Rattray, 2008). Further, excess of corticosterone (CORT), the major GC in rodents, inhibits neuronal differentiation in the hippocampus (Wong and Herbert, 2006) and GCs affect the migration of post-mitotic neurons during the development of the cerebral cortex (Fukumoto et al., 2009). It has been reported that AChRs modulate neuron differentiation (Takarada et al., 2012) and that AChRs are differentially expressed during PC12 differentiation (Nery et al., 2010).

The aim of the present work was to study the chronic effect of CORT on the differentiation of a neuronal cell line exhibiting a cholinergic phenotype (Allen et al., 2000). Using fluorescence microscopy, quantitative-PCR, cell-cycle analysis and electrophysiology, we determined that CORT impairs the differentiation process through modulation of AChR expression and function.

EXPERIMENTAL PROCEDURES

Cell culture and CORT treatment

For standard growth conditions, CNh cells were plated in Petri dishes and maintained in feeding medium consisting of DMEM/Ham F12 nutrient mixture (1:1) supplemented with 10% bovine serum, 2.5% fetal bovine serum, 100 U/mL penicillin, 100 μg/mL streptomycin (Sigma, St. Louis, MO, USA), *complete medium*. For differentiation, the cells were kept in differentiating medium consisting of DMEM/Ham F12 (1:1), where the adult bovine serum concentration was decreased from 10% to 3% and fetal bovine serum was omitted. CORT (Sigma) was added at the beginning of the differentiation protocol and replenished with fresh CORT after 48 h in culture. Ethanol was used as vehicle and was kept below 0.04% in all cases. Control cells were incubated in the presence of the vehicle.

Transfections

CNh cells were transfected with 0.5-μg/μl of α7-GFP plasmid (kindly provided by Dr. S. Heinemann, Salk Institute, CA) or e-GFP plasmid (kindly provided by Dr. F. Ceriani, Fundación Instituto Leloir-CONICET, Argentina) as controls. Transient transfections were performed with Lipofectamine 2000 (Invitrogen, Carlsbad, CA, USA) following instructions provided by the manufacturer. Eighteen hours after transfection, cells were transferred to differentiation medium, left untreated or treated with 1 μM CORT for 48 h and subsequently harvested for examination of the cell cycle by flow cytometry.

Fluorescence microscopy

To visualize total α7- and α4-AChR, CNh cells grown on coverslips were washed with phosphate-buffered saline (PBS; 150 mM NaCl, 10 mM Na_2HPO_4, 10 mM, NaH_2PO_4, pH 7.4), fixed with 4% paraformaldehyde, permeabilized with 0.1% Triton X-100, and stained with mAb306 (1/1000, kindly provided by Dr. J. Lindstrom, Perelman School of Medicine, University of Pennsylvania, PA) for α7-AChR or mAb299 (1/100, Sigma) for α4-AChR overnight at 4 °C. Next, the cells were labeled with Texas Red-goat anti-rabbit IgG (kindly provided by Dr. T. Santa Coloma, Institute of Biomedical Research UCA-CONICET, Argentina) for 2 h at room temperature (RT). To observe the cell-surface α7-AChRs, cells were incubated with mAb306 in the growth medium for 1 h at 4 °C, fixed and labeled with Texas Red-goat anti-mouse IgG for 1 h at RT. They were then mounted in 90% glycerol in PBS and examined with a Nikon Eclipse E-600 or E-300 fluorescence microscope (Nikon, Melville, NY, USA). Images were captured using a K2E Apogee CCD camera driven by CCDOPS software (Santa Barbara Instrument Group, Santa Barbara, CA, USA) or a Hamamatsu ORCA-ER CCD camera driven by a Metamorph package (Meta Imaging Software, Downingtown, PA, USA), respectively. For preparation of membrane sheets, CNh cells grown on coverslips were disrupted as previously described (Borroni et al., 2007) using a single (100–300 ms) ultrasound pulse in KGlu buffer (20 mM Hepes, pH 7.2, containing 120 mM potassium glutamate and 20 mM potassium acetate). The resulting membrane sheets were then fixed and labeled for α7-AChR as mentioned above. Imaging was performed in PBS containing 25-μg/ml of a saturated trimethylammonium-DPH solution in order to identify and record membrane sheets in the blue channel, thus avoiding biased selection based on staining intensities in the red (Texas Red-goat anti-mouse IgG) channel. Membrane sheets were mounted and examined as described above.

Quantitative fluorescence microscopy analysis

To ensure objectivity, all measurements were performed on coded slides, under blind conditions, carrying out the measurements of the different conditions with the same standardized observation scheme. Fluorescence images were analyzed with the ImageJ software (National Institutes of Health, Bethesda, MD, USA). The average fluorescence intensity over different areas of the cell surface or whole cells was calculated for each experimental condition from cells randomly chosen under phase contrast or in the blue (UV) channel in the case of membrane sheets. Fluorescence intensities were measured from 16-bit images by delimiting membrane areas (membrane sheets) or the whole cell (total and plasma membrane AChRs) in 10–30 different fields for each experimental condition. Fluorescence intensity values were corrected for fluorescence background measured in areas adjacent to the cells. Results were expressed as the average ± SEM of three or more independent experiments.

Western blot analysis

Cells were scraped and resuspended in radioimmunoprecipitation assay (RIPA) buffer (50 mM Tris-HCl, pH 7.4; 150 mM NaCl; 1 mM EDTA; 1% Triton X-100; 1% Sodium deoxycolate; 0.1% SDS; 1% protease inhibitors). The samples were centrifuged at 4 °C to remove debris. The supernatant was resuspended in Laemmli's buffer, loaded onto 12.5% polyacrylamide gels and submitted to electrophoresis.Samples were transferred to Immobilon membranes (Millipore Corporation, Billerica,

MA, USA) and the proteins were revealed by immunoblotting. We used mAb319 (a gift of Dr. J. Lindstrom, Perelman School of Medicine, University of Pennsylvania, PA, USA) to detect α7-AChR and mouse anti-actin (provided by Dr. T. Santa Coloma, Biomedical Research Institute, UCA-CONICET, Argentina) to detect actin. Chemiluminescence was detected with ECL (Amersham Bioscience). Quantification of bands was performed using Image J. The expression levels of α7-AChR proteins were normalized to endogenous actin.

RNA isolation, reverse transcription, end point PCR (PCR) and real time PCR (qPCR) analysis

Total RNA was isolated from 1×10^6 cells using the Quick-Zol kit (Kalium Technologies, Bernal, Buenos Aires, Argentina). mRNA was converted into cDNA using the Molony Murine Leukemia virus reverse transcriptase (MLV-RT; Promega, Madison, WI, USA) and random primers (Promega, USA).

End-point PCR was run in a Mini Cycler(MJ Research, Waltham, MA, USA). Semiquantitative PCR analysis was carried out by using GAPDH mRNA amplification as an internal standard. PCR products were analyzed by electrophoresis on a 1.5% agarose gel stained with ethidium bromide.

Relative quantification of mRNA by qPCR was performed using a Rotor-Gene 6000 (Corbett Research, Sydney, Australia). The primer sequences for end-point PCR and qPCR were: α7-AChR, sense 5′-CTGATG GTGGCAAAATGCC-3′ and antisense 5′-GGCCTCGGA AGCCAATGTAG′3′, GAPDH sense 5′-TTCACCACCATG GAGAAGGC-3′ and antisense 5′-AGTGATGGCATGG ACTGTGGTC-3′. The comparative CT method was used to determine the relative gene expression (Livak and Schmittgen, 2001; Schmittgen and Livak, 2008). CT values of target mRNA were normalized with the CT value of the housekeeping gene GAPDH using the formula $\Delta CT = CT\ (target) - CT\ (GAPDH)$ and the data are presented as $2^{-\Delta CT}$. The method was further used to determine the relative expression of the same gene from two samples: $\Delta\Delta CT = \Delta CT\ (sample\text{-}A) - \Delta CT\ (sample\text{-}B)$. Data are presented as $2^{-\Delta\Delta CT}$ (Schmittgen and Livak, 2008).

Morphometric analysis

In order to quantify the morphological changes undergone by CNh cells in differentiation medium, we established different stages of CNh development. The proportion of cells in each stage of development (1–5, 1 being the least developed) in differentiation media (Fig. 3A, B) was thus followed on a standardized arbitrary basis. Cells were imaged with a 10× phase contrast objective and ten representative images of random fields were taken from control and CORT-treated cells at day 4 in differentiation media. Approximately five hundred cells were blindly (see above) analyzed for each condition/experiment.

Cell-cycle analysis

About 1×10^6 cells grown on 6-cm Petri dishes were washed twice with PBS and subsequently fixed with ice-cold ethanol 70% (v/v) (3 ml were added drop-wise). Cells were maintained at 4 °C overnight to complete fixation. Cells were subsequently washed twice with PBS, resuspended in 1 ml PBS containing 100-μg/ml of RNAse and 40-μg/ml propidium iodide (PI; Sigma), and incubated in the dark for 15 min at RT. Finally, the samples were analyzed with a FACS Calibur cytometer (BD Biosciences, San Jose, CA, USA). Data analysis was carried out with BD Cell Quest Pro software (BD Biosciences).

Cell proliferation studies

1×10^5 CNh cells were seeded in 35-mm plates and treated with 1 μM CORT or 10 μM methyllycaconitine (MLA) (control cells were treated with vehicle, ethanol or PBS, respectively). After 24 h, 5-bromo-2′-deoxyuridine (BrdU, 1 mg/ml; kindly provided by Dr. A. Schinder, Fundación Instituto Leloir, Buenos Aires, and Drs. N.P. Rotstein and L.E. Politi, INIBIBB, Bahía Blanca, Argentina) was added to the cell culture medium at a final concentration of 0.03 mg/ml. After 6 h of incubation at 37 °C in a 5% CO_2 atmosphere, the medium was replaced with fresh medium. 18 h later, cells were washed with PBS and fixed as above. Cells were then treated with 2 M HCl for 20 min at RT, washed with PBS, permeabilized with 0.2% Triton-X100 for 5 min and stained with anti-mBrdU (1/200) overnight at 4 °C. Then, cells were labeled with Cy2-anti-mouse IgG (Jackson, West Grove, PA, USA) 2 h at RT. To observe the nuclei, cells were incubated with 0.035 mg/ml PI or Hoechst (Sigma) in PBS for 15 min at RT. Finally, cells were mounted and imaged as above. For quantification of the $BrdU^+$ incorporation index, at least 1500 cells were counted in total from three independent experiments.

MTT assay

Cell proliferation was estimated by the MTT (kindly provided by Dr. M.I. Aveldaño, INIBIBB, Bahía Blanca) reduction assay (Mosmann, 1983). After treatments, MTT (5 mg/ml) was added to the cell culture medium at a final concentration of 0.5-mg/ml. After incubating the plates for 30 min at 37 °C in a 5% CO_2 atmosphere, the assay was stopped. The cells were washed with PBS and solubilized with acid isopropyl alcohol. The extent of MTT reduction was measured at 570 nm with a spectrophotometer. Results were expressed as a percentage of the control.

Electrophysiology

CNh cells were plated on circular coverslips (12 mm diameter) and maintained either under control conditions or in the presence of CORT for 48 h as described above. For electrophysiological recordings, the cells were changed to HBS solution containing (mM): 150 NaCl, 3 KCl, 3 CaCl2, 2 MgCl2, 5 HEPES, 5 HEPES-Na and 5 Glucose, 300 mOsm. They were then placed on the recording chamber under constant perfusion with HBS. Recordings were made at RT using microelectrodes (4–6 Mohms) pulled from borosilicate

glass (KG-33; King Glass, Claremont, CA, USA) and filled with (mM): 120 K-gluconate, 20 KCl, 5 NaCl, 4 MgCl2, 0.1 EGTA, 10.0 HEPES, 4.0 Tris-ATP, 0.3 Tris-GTP and 10 phosphocreatine, pH 7.3, 290 mOsm. Recordings were obtained using an Axopatch 200B amplifier (Molecular Devices, Sunnyvale, CA, USA), digitized (Digidata 1322A; Molecular Devices), and acquired at 20 kHz onto a personal computer using the p-Clamp 9 software (Molecular Devices). Whole-cell voltage-clamp recordings were performed at a holding potential of −60 mV. In all records, series resistance was 10–20 Mohm and leak current was < 100 pA at holding potential. Membrane capacitance and input resistance were obtained from current traces evoked by a hyperpolarizing step of 10 mV. To test the membrane expression of AChRs on CNh cells, a puff of 50 μM nicotine (Sigma–Aldrich) was applied by air pressure (5–10 psi, 20 ms) using a Picospritzer (Parker Hannifin Corp, Cleveland, OH, USA) and changes in the membrane current were monitored in voltage-clamp mode. Peak amplitudes of evoked currents were calculated from the average of 5–10 traces.

Statistical analysis

Total AChR, α7-AChR mRNA levels and cell-cycle parameters were analyzed by a two-way analysis of variance (ANOVA) in order to evaluate the effects of CORT treatment, differentiation day, nicotine, α7AChR-GFP over-expression and possible interactions between factors. When significant interactions were found (α7AChR-GFP over-expression), simple effects ANOVA was used. Tukey's or Bonferroni post hoc test was performed to test differences between more than two groups. $BrdU^+$ relative index, nicotine-evoked currents and α7AChR levels at the plasma membrane were analyzed by Student's *t* test. Morphometric studies were subjected to X^2 analysis to assess the significance in both distributions. All results are presented as mean ± SEM. The observed differences were considered to be statistically significant when $p < 0.05$. Analysis of data was performed using SPSS version 21.0 and Origin version 8 OriginLab Graphing Software.

RESULTS

CORT negatively affects the expression of α7- and α4-AChR in the CNh cell line

In order to analyze whether chronic treatment with CORT affected the biology of neuronal AChRs, CNh cells were incubated with 1 μM CORT for 2, 4 and 7 days (T2, T4 and T7, respectively) and the expression levels of the nicotinic α_7 and α_4 AChR-subunits were analyzed by immunofluorescence. Briefly, CNh cells were grown for 48 h in complete medium (10% bovine serum, 2.5% fetal bovine serum) and then maintained in differentiation medium (3% bovine serum) for the indicated periods in the presence of CORT. As shown in Fig. 1, the expression of α7-AChR changed along differentiation [two-way ANOVA: $F = 4.51$ $p = 0.0217$ for days factor effect], with a significant drop at T2 (control T2: 67.4 ± 8.9, $n = 4$; values represent mean (% with respect to undifferentiated cells, T0) ± SEM), followed by a recovery at T4 (control T4: 95.8 ± 8.0, $n = 4$) and T7 (control T7: 95.4 ± 9.5, $n = 4$). Treatment with CORT reduced the expression of α7-AChR by ∼40% at all days tested (control: 93.9 ± 8.6, CORT: 59.5 ± 3.4, $n = 12$; two-way ANOVA: $F = 18.93$ $p = 0.0002$ for CORT treatment factor effect). These results were confirmed by western blot analysis (Fig. 1C, control T4: 100.0 ± 6.2, CORT T4: 74.7 ± 7.9 $n = 4$; Student's *t* test, $p = 0.040$) employing another α7-AChR antibody, mAb319.

To gain further insight into the changes in α7 protein expression, we quantified the changes at the mRNA level. As shown in Fig. 1D, the expression of α7-AChR mRNA changed along differentiation in a similar way to that of the protein [two-way ANOVA: $F = 8.80$ $p = 0.0180$ for day factor effect]. In the absence of the steroid, mRNA levels decreased at T2 (control T2: 0.66 ± 0.11, $n = 3$) and increased at T4 (control T4: 2.03 ± 0.45, $n = 3$) with respect to the mRNA level at T0. Treatment with CORT suppressed the expression of α7-AChR mRNA at all tested days [two-way ANOVA: $F = 33.60$ $p = 0.0004$ for CORT treatment factor effect).

Protein expression of the α4-AChR subunit was also examined by fluorescence microscopy. CORT was also found to decrease the expression of the AChR containing an α4 subunit (control: 138.3 ± 11.6, CORT: 99.0 ± 22.8, $n = 12$; two-way ANOVA: $F = 7.55$ $p = 0.0132$ for CORT treatment factor effect], albeit to a lesser extent than that of α7-AChR (Fig. 2).

CORT affects the differentiation of CNh cells

After chronic treatment with CORT, CNh cells did not reach a mature morphology. In order to quantitatively analyze this effect, we first defined different stages of development of CNh cells, as described in Section 'Morphometric analysis'. As shown in Fig. 3A, a careful evaluation of cell morphology by phase contrast microscopy at day four of differentiation revealed that the majority of control CNh cells remained at stages 2 and 3. In contrast, CORT-treated cells remained principally at stage 1, showing an undifferentiated phenotype, which reached about 35% in CORT-treated cells (Fig. 3B). We also observed a reduction at stage 3 (Fig. 3B) in CORT-treated cells with a consequent decrease in the differentiated phenotype. X^2 analyses ($p < 0.05$) indicated differences between the two populations. CORT-treated cells at T4 exhibited a degree of differentiation equivalent to undifferentiated cells at T0 (data not shown). These results suggest that CORT impairs or delays cell differentiation in CNh cells.

To confirm that CORT affects the differentiation of CNh cells, we resorted to cell-cycle analysis. Cells were labeled with PI and studied by flow cytometry (Fig. 3C). As shown in Fig. 3C, when CNh cells were changed to differentiation medium they remained arrested mainly in G0/G1 (control: 69.1 ± 2.3, CORT: 59.0 ± 1.3, $n = 12$; two-way ANOVA: $F = 19.22$ $p = 0.0004$ for CORT treatment factor effect). The dotted gray line denotes the G0/G1 level in undifferentiated CNh cells (data not

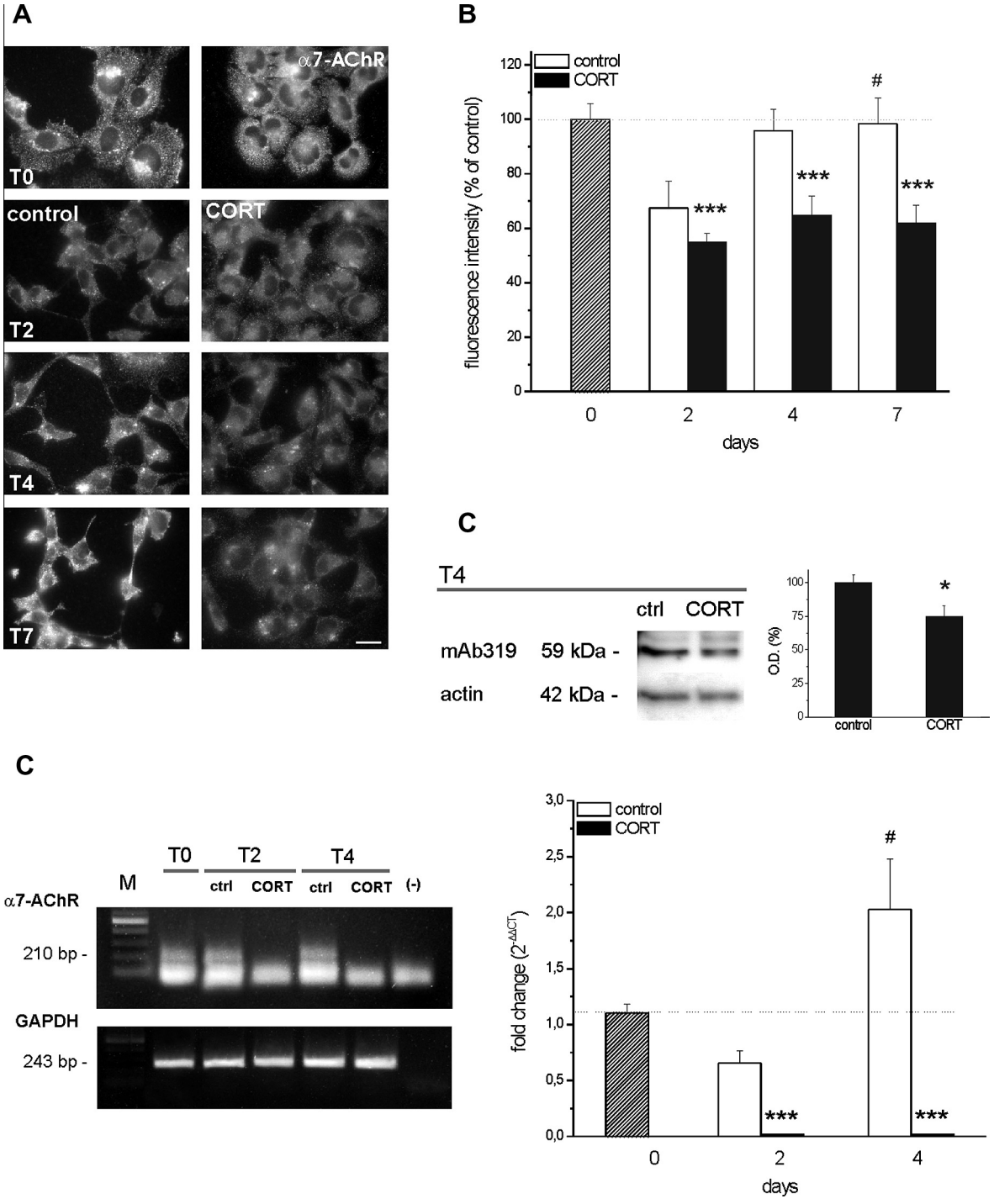

Fig. 1. CORT negatively affects the expression of α7-AChR in CNh cells. (A) Representative immunofluorescence images of CNh cells treated with 1 μM CORT for different times. Control cells were treated only with the vehicle. At different days cells were fixed and stained with α7-AChR specific antibody (mAb306). Bar: 20 μm. (B) Graph showing the quantification of fluorescence intensity of α7-AChRs relative to undifferentiated cells (column at T0). Results are expressed as mean ± SEM of at least three independent experiments. Two-way ANOVA followed by main effects analyses: $p < 0.001$ for treatment factor effects; $p < 0.05$ for day factor effects; $n = 4$. (C) Analysis of the levels of α7-AChR protein in CNh cells differentiated for 4 days (T4), treated with 1 μM CORT. Control cells received only the drug vehicle. Protein levels were determined by Western blot analysis. Graph show normalized α7-AChR / actin ratios in control and CORT-treated cells. Student's *t* test, $p < 0.05$; $n = 3$. (D) *Left,* Agarose gel electrophoresis of the PCR reaction products. Transcripts of α7-AChR and GAPDH were detected as bands of 210 and 243 bp respectively. M: DNA marker (100 bp ladder), *Right*, Relative expression of α7-AChR mRNA during 1 μM CORT exposure of CNh cells. The fold change of α7-AChR was calculated using $2^{-\Delta\Delta CT}$. α7-AChR mRNA expression was referred to GAPDH gene and compared to the calibrator (T0) (See Methods). Results are expressed as mean ± SEM of at least three independent experiments. Two-way ANOVA followed by main effects analyses: $p < 0.001$ for CORT treatment factor effects; $p < 0.05$ for day factor effects; $n = 3$). (*) Denotes statistically significant differences between control and CORT groups; (#) denotes statistically significant differences within the control group. The presence of one, two or three symbols indicate p values < 0.05, < 0.01 and < 0.001, respectively.

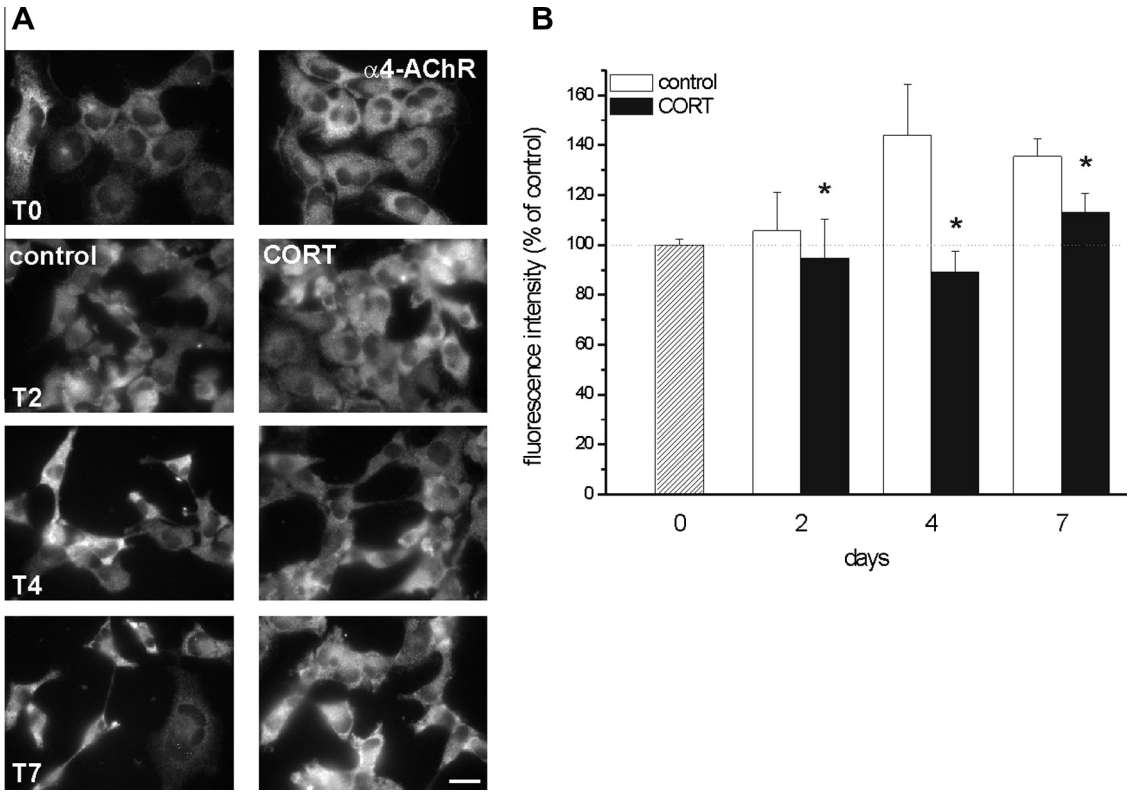

Fig. 2. CORT affects the expression of α4-AChR in CNh cells. (A) Representative immunofluorescence images of CNh cells treated with 1 μM CORT for different periods of time. Control cells were treated only with the vehicle. At the days noted, cells were fixed and stained with α4-AChR specific antibody (mAb299). Scale bar = 20 μm. (B) Graph showing the quantification of fluorescence intensity of α4-AChRs relative to undifferentiated cells (column at T0). Results are expressed as mean ± SEM of at least three independent experiments. Two-way ANOVA followed by main effects analyses: $p < 0.05$ for CORT treatment factor effects; $n = 4$). (*) denotes statistically differences between control and CORT groups ($p < 0.05$).

shown). In contrast, cells treated with CORT prolonged their G2/M phase, still remaining as undifferentiated cells after T7 (Fig. 3D) (control: 22.6 ± 1.7, CORT: 35.4 ± 1.8, $n = 12$; two-way ANOVA: $F = 34.41$ $p = 0.00001$ for CORT treatment factor effect). For the S phase we found an effect by day factor (two-way ANOVA: $F = 32.25$ $p = 0.00001$ for day factor effect), but no effect by the CORT treatment factor. For both control and CORT cells, there were differences in the S phase at T4 ($p < 0.001$ T2 vs. T4) and T7 ($p < 0.00001$ T2 vs. T7) with respect to T2. These results show that CORT affects the cell cycle of CNh cells, shifting them to a more undifferentiated stage.

AChRs are involved in the differentiation of CNh cells

In order to evaluate whether AChRs are involved in the differentiation process of CNh cells, we treated these cells with 50 μM nicotine from the beginning of the differentiation process, and then analyzed the stage of their cell cycle by flow cytometry. We used T2 in subsequent experiments as T2 marks the beginning of differentiation (arrest in G0/G1 phase, Fig. 3C). As shown in Fig. 4A, nicotine treatment dramatically altered all cell-cycle parameters when the cells were analyzed at T2. It was possible to determine that CORT treatment affected differentiation in the G0/G1 phase (two-way ANOVA: $F = 16.41$ $p = 0.0037$ for CORT treatment factor effect), also in the presence of nicotine (two-way ANOVA: $F = 23.78$ $p = 0.0012$ for nicotine factor effect). For the S phase we found an effect by CORT treatment factor (two-way ANOVA: $F = 25.02$ $p = 0.0011$ for CORT treatment factor effect). Similarly, for the G2/M phase we found an effect by the CORT treatment factor (two-way ANOVA: $F = 29.53$ $p = 0.0006$ for CORT treatment factor effect) and for the presence of nicotine (two-way ANOVA: $F = 26.62$ $p = 0.0009$ for nicotine factor effect). Furthermore, in the presence of nicotine, CNh cells were less differentiated, i.e., they exhibited a decrease in the G0/G1 phase (control: 65.2 ± 0.8, control + nicotine: 59.5 ± 2.6, $n = 3$) and a concomitant increase in the G2/M phase (control: 26.27 ± 0.9, control + nicotine: 32.94 ± 2.7, $n = 3$), thus resembling CORT-treated cells (CORT: 33.4 ± 1.7, $n = 3$) (Fig. 4A). Interestingly, when nicotine was incubated together with CORT, a synergistic effect was observed on the cell cycle, as evidenced by the decreased cell arrest in the G0/G1 phase (CORT: 60.7 ± 0.7, CORT + nicotine: 52.7 ± 0.3, $n = 3$) and a further increase in the G2/M phase (CORT + nicotine: 43.0 ± 0.9, $n = 3$) (Fig. 4A). These results indicate that AChRs participate in the differentiation of CNh cells, and that CORT acts at least in part through these receptors, eventually affecting the cell-cycle signaling pathway.

CORT enhanced CNh cells proliferation

In order to evaluate whether the undifferentiated CNh cells were in a proliferative state as a consequence of

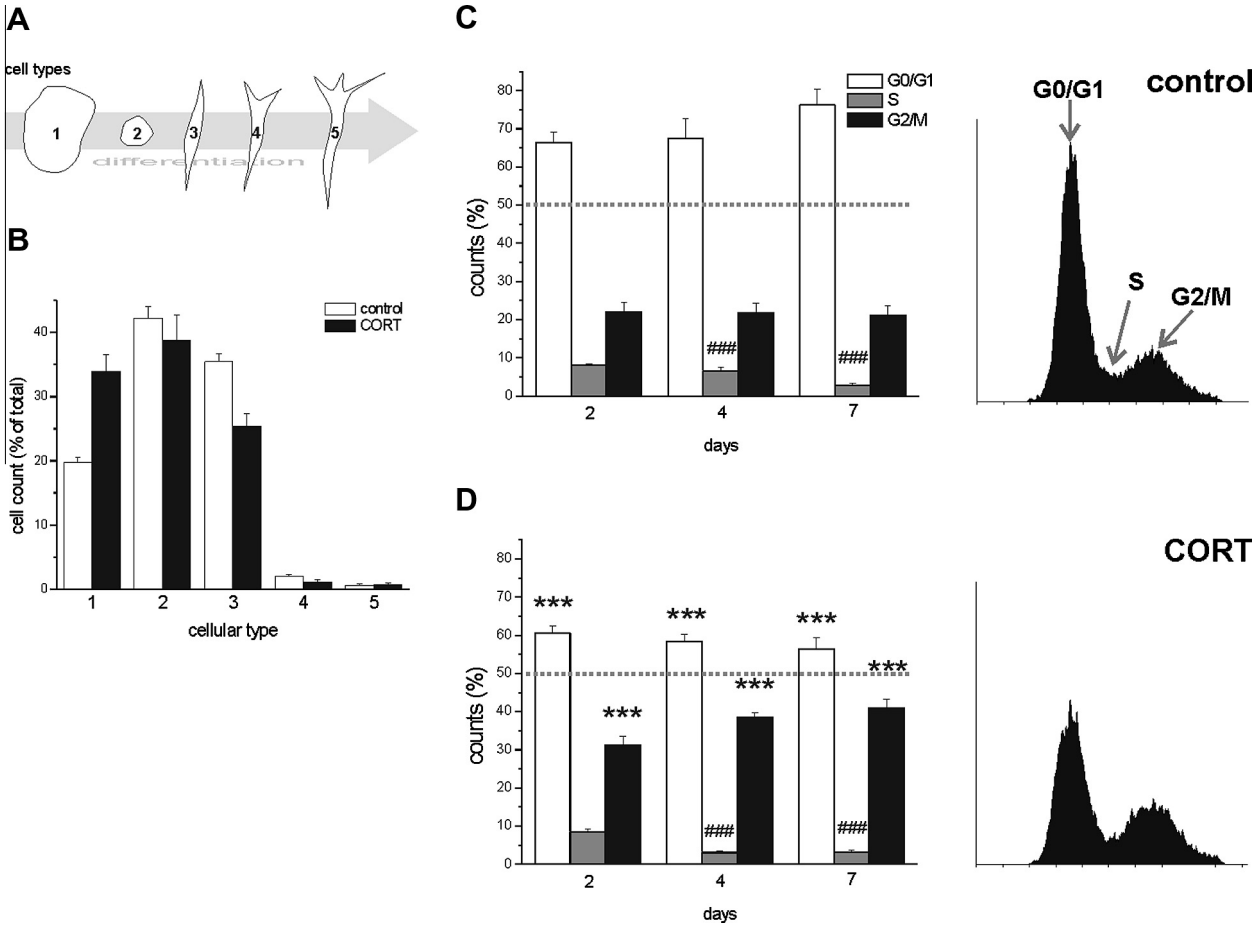

Fig. 3. CORT-treated cells remain in an undifferentiated state. (A) Scheme of cell-cycle progression in differentiated CNh cells through several days in differentiation medium. (B) Histogram representing the stage distribution at T4 of control and CORT-treated cells. Control cells received only the drug vehicle. X^2 analyses denote $p < 0.05$ between both distributions. (C) Representative histogram of cell cycle in control and (D) 1 μM CORT-treated CNh cells. Results are expressed as mean ± SEM of at least three independent experiments. Two-way ANOVA followed by main effects analyses: G0/G1, $p < 0.001$ for CORT treatment factor effects; S, $p < 0.00001$ for day factor effects; G2/M, $p < 0.0001$ for CORT treatment factor effects; $n = 3$). Left panels show representative cell-cycle distribution at T4 of each condition. (*) Denotes statistically significant differences between control and CORT groups (for each phase, respectively); (#) denotes statistically differences within control or CORT group. The presence of three symbols indicates p values < 0.001.

the CORT treatment, we calculated BrdU incorporation as a measure of cell proliferation in control and CORT-treated cells at T2 (Fig. 5A, B). We found that the $BrdU^+$ incorporation index was higher by 2.3-fold in CORT-treated cells ($BrdU^+$ incorporation index: control 23.8 ± 1.8, CORT 55.9 ± 4.3; Student's t test, $p = 0.0024$, $n = 3$).

Additionally, we calculated a proliferation index (S phase plus G2/M phase) as in Wang et al. (2011). For the proliferation index we found an effect by the CORT treatment factor (two-way ANOVA: $F = 16.46$ $p = 0.0037$ for treatment factor effect) and for the presence of nicotine (two-way ANOVA: $F = 23.82$ $p = 0.0012$ for nicotine factor effect). As shown in Fig. 5C, CORT treatment significantly increased the proliferation index (CORT: 39.3 ± 0.7, $n = 3$) compared to control cells (control: 34.8 ± 0.8, $n = 3$). Nicotine treatment increased the proliferative index in control (control + nicotine: 40.5 ± 2.6, $n = 3$) and even more so in CORT-treated cells (CORT + nicotine: 47.3 ± 0.3, $n = 3$) (Fig. 5C). We complemented this study with the MTT assay, which has been used to estimate the proliferative state of cells (Mosmann, 1983). We found an effect in the MTT reduction as consequence of CORT treatment (two-way ANOVA: $F = 14.40$ $p = 0.0026$ for CORT treatment factor effect). Cells treated with CORT and CORT plus nicotine were found to exhibit a higher degree of proliferation (~50%) than untreated cells at T2 (Fig. 5D).

Overexpression of GFP-tagged α7-AChR abolishes the effects of CORT on the cell cycle

As shown in Fig. 1, the expression levels of α7-AChR were reduced by about 40% as a consequence of CORT treatment. In order to analyze whether this subtype of receptor was specifically involved in a cell-cycle defect triggered by CORT, we overexpressed α7-AChR-GFP plasmid or eGFP as a control in CNh cells and analyzed the cell cycle under different conditions. As shown in Fig. 6, the control transfection procedure with eGFP plasmid alone did not modify the cell cycle at T2: ~65% of control cells remained in G0/G1 (control-GFP: 66.7 ± 2.7, CORT-GFP: 57.9 ± 1.6, $n = 4$–5; two-way ANOVA followed by main effects analyses:

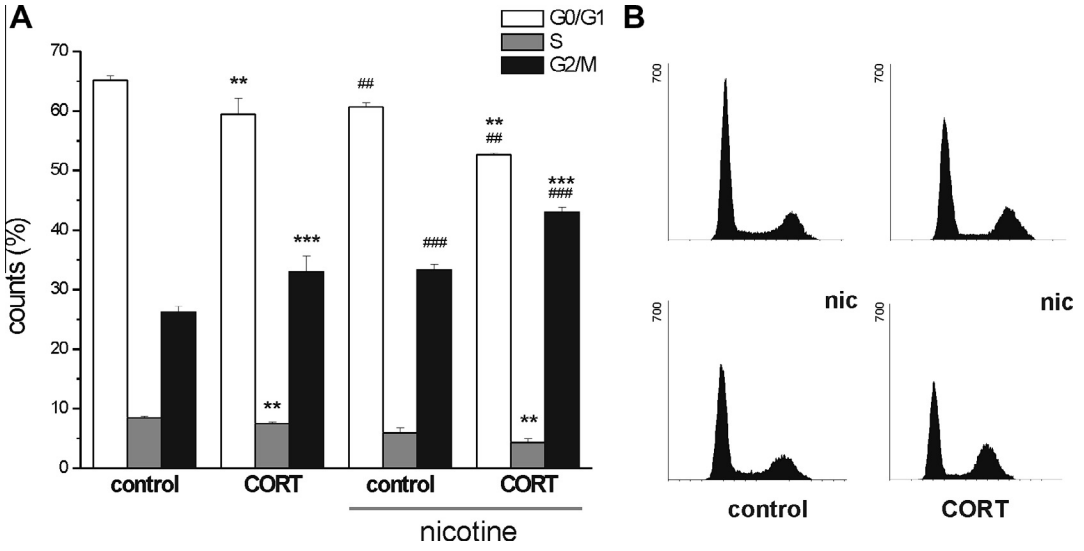

Fig. 4. Nicotine treatment modified the cell cycle in CNh cells. (A) Representative histograms of cell cycle in control and 1 μM CORT-treated cells with or without 50 μM nicotine (nic). Results are expressed as mean ± SEM of at least three independent experiments. Two-way ANOVA followed by main effects analyses: G0/G1 phase, $p < 0.01$ for CORT treatment factor effects, $p < 0.01$ for nicotine factor effects; S phase, $p < 0.01$ for CORT treatment factor effects; G2/M phase, $p < 0.001$ for CORT treatment factor effects, $p < 0.001$ for nicotine factor effects; $n = 3$). (*) Denotes statistically significant differences consequence of CORT treatment (for each phase, respectively); (#) denotes statistically significant differences resulting from nicotine treatment. The presence of two or three symbols indicate p values < 0.01 and < 0.001, respectively. (B) Representative histograms of cell cycle of CNh cells at T2 in control and 1 μM CORT-treated cells with or without 50 μM nicotine (nic).

$F = 10.04$ $p = 0.009$). Overexpression of α7-AChR-GFP did not modify the cell cycle in control cells but abolished the effects of CORT on the cell cycle (control-α7-AChR-GFP: 63.7 ± 2.5, CORT-α7-AChR-GFP: 67.3 ± 1.3, $n = 4$–5. In order to evaluate whether the α7-AChR was specifically involved in the proliferation of CNh cells, we resorted to BrdU incorporation as a measure of cell proliferation in control and CNh cells treated with the specific α7-AChR inhibitor, MLA, at T2 (Fig. 6C, D). The $BrdU^+$ incorporation index was found to be ∼34% higher in MLA-treated cells ($BrdU^+$ incorporation index: control 33.2 ± 1.0, MLA 44.5 ± 3.8; Student's t test, $p = 0.0292$, $n = 4$). These results strongly suggest that CORT induces cell-cycle progression through the α7AChR or that this AChR subtype is able to rescue the cell-cycle alterations provoked by CORT treatment.

CORT treatment inhibits nicotine-evoked currents in CNh cells

It is a well-established fact that hydrocortisone reversibly and noncompetitively suppresses AChR response in rat superior cervical ganglion cells (Uki et al., 1999). Moreover, studies have shown that CORT inhibits AChRs in PC12 cells in a noncompetitive manner (Shi et al., 2002). To further examine whether chronic treatment with CORT inhibits AChR function during differentiation, CNh cells were differentiated for two days in the presence of CORT, and their ability to evoke ionic currents was analyzed after puff application of 50 μM nicotine (Fig. 7). Whole-cell voltage-clamp recordings in CNh control and CORT-treated cells showed no difference in intrinsic membrane properties (input resistance 487.6 ± 100.5 MΩ vs. 318.6 ± 70.7 MΩ, $p = 0.23$; resting potential −49.9 ± 2.6 mV vs. −50.7 ± 3.9 mV, $p = 0,87$; and capacitance 35.9 ± 6.0 pF vs. 33.6 ± 5.5 pF; with $n = 12$ for control and $n = 8$ for CORT). Moreover, a transient inward current in response to nicotine application was observed in control cells (Fig. 7A, B). However, chronic treatment with CORT for two days markedly reduced the peak amplitude of the nicotine-evoked currents (control: 27.6 ± 6.0, $n = 12$; and CORT: 1.92 ± 2.23, $n = 8$; $p = 0.0033$) (Fig. 7A, B). These results confirm that chronic treatment with CORT down-regulates AChRs and in turn abolishes the nicotinic response, thus indicating a putatively cholinergic mechanism underlying the CORT-related cell-cycle arrest described herein.

CORT impairs the plasma membrane expression of α7-AChR in CNh cells

An alternative mechanism by which CORT induces cell-cycle arrest might be the impairment of α7-AChR cell-surface expression, affecting AChR signaling. To test this, the plasma membrane expression of α7-AChR was measured in cells treated with CORT at T2. Two different fluorescence microscopy approaches were employed in order to study the surface localization of α7-AChR. As shown in Fig. 8, the plasma membrane expression of α7-AChR in CNh cells decreased by ∼25–30% after CORT treatment (control: 100.0 ± 6.4, CORT: 74.4 ± 4.7, $n = 3$; Student's t test, $p = 0.03$). Similar results were observed using unroofed plasma membrane sheets: membrane sheets from CORT-treated cells had 50% lower levels of α7-AChR with respect to control cells (control: 100.0 ± 10.1, CORT: 48.1 ± 6.2; $n = 3$; Student's t test, $p = 0.01$). These results indicate that CORT impairs the expression of α7-AChR and its cell surface delivery. Although this could be an additional mechanism of down-regulation of α7-AChR signaling, it falls short of explaining the ∼95%

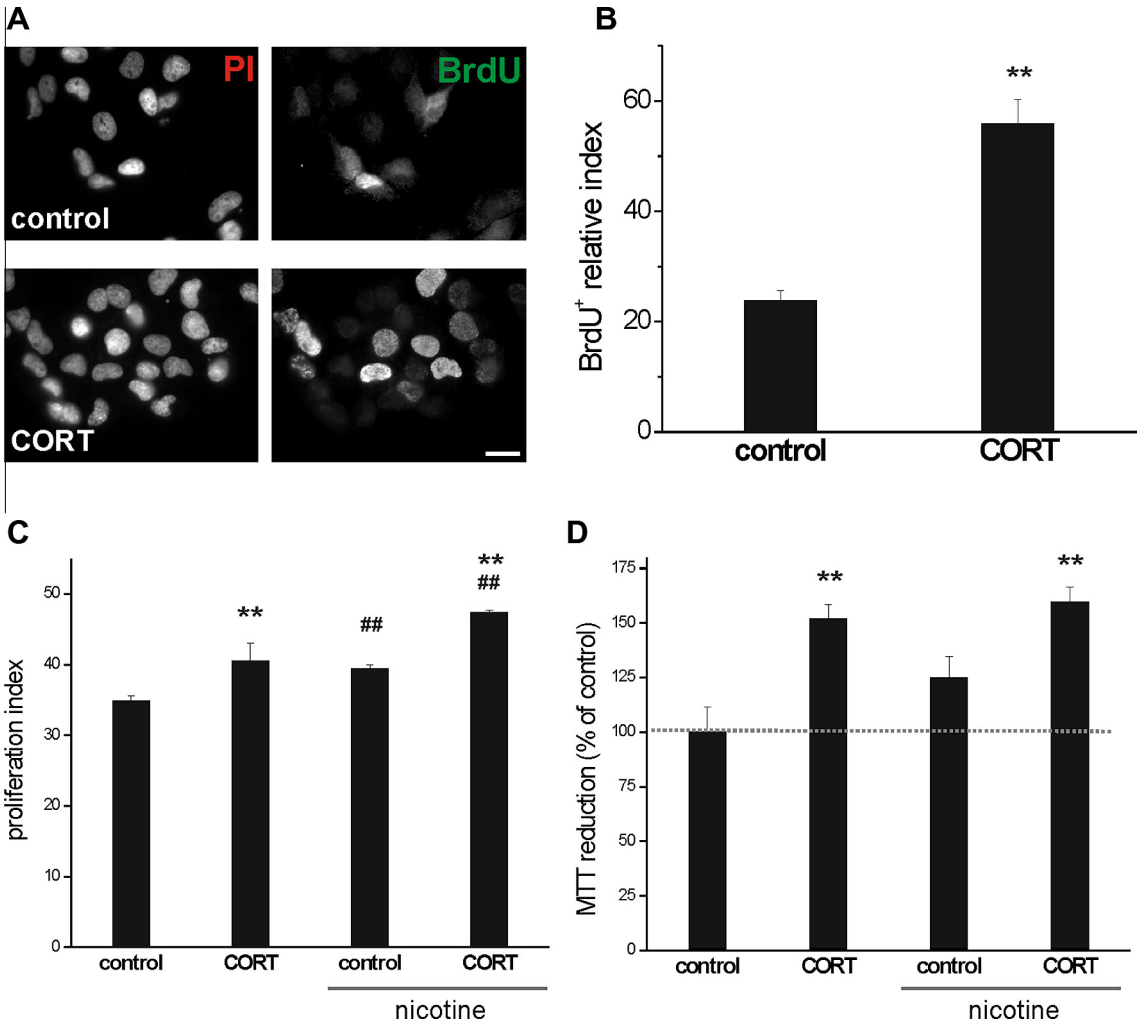

Fig. 5. CORT treatment promotes cell proliferation in CNh cells. (A) Representative immunofluorescence images of CNh cells treated with 1 μM CORT (control cells were treated only with the vehicle) at T2 showing PI and BrdU labeling. Bar: 20 μm. (B) Estimation of the $BrdU^+$ proliferation index for control and CORT-treated cells at T2. $BrdU^+$ proliferation index was calculated as the proportion of $BrdU^+$ cells to total cells in each field (nucleus labeled with PI). At least 1500 cells were counted in each case. Results are expressed as mean ± SEM of at least three independent experiments. Student's *t* test, $p = 0.0024$. (C) Proliferation index (S phase + G2/M phase (Wang et al., 2011)) estimated for control and 1 μM CORT-treated cells in the presence, or not, of 50 μM nicotine. Results are expressed as mean ± SEM of at least three independent experiments. Two-way ANOVA followed by main effects analyses: $p < 0.01$ for CORT treatment factor effects, $p < 0.01$ for nicotine factor effects; $n = 3$. (D) Proliferation estimated by MTT reduction assay. Results are expressed as a percentage of the control and represent mean ± SEM of at least three independent experiments. Two-way ANOVA followed by main effects analyses: $p < 0.01$ for CORT treatment factor effects; $n = 4$). (*) Denotes statistically significant differences as a consequence of CORT treatment; (#) denotes statistically significant differences resulting from nicotine treatment. The presence of two symbols indicates *p* values < 0.01.

decrease in α7-AChR function observed in the electrophysiological experiments (Fig. 7).

DISCUSSION

Stress contributes to a number of brain disorders and various studies have shown the relationship between stress and AChRs (reviewed in (Hunter, 2012)). It has been reported that AChRs are important mediators of adaptation to stress in a number of brain regions (Hunter, 2012). However, the molecular and cellular mechanisms behind these observations are still unknown.

In this work we show that chronic CORT treatment prevents CNh cells from acquiring a mature phenotype, manifested in a decrease in the G0/G1 phase and an increase in proliferation. This phenomenon is mediated by the interaction or modulation of CORT with the AChR. Additionally, the CORT-induced cell-cycle alterations were rescued by α7-AChR overexpression and the CORT effect could be mimicked by employing the α7-AChR specific inhibitor MLA. These findings indicate that AChRs, and the α7-AChR subtype in particular, are required for the acquisition of a mature cell phenotype in the CNh neuronal cell line, and thus the absence of the AChR protein from the plasma membrane, or its dysfunction, would result in impairment of cell differentiation.

GC acts over GC receptors which are expressed throughout the brain. These receptors could function as transcription factors and then regulate gene expression,

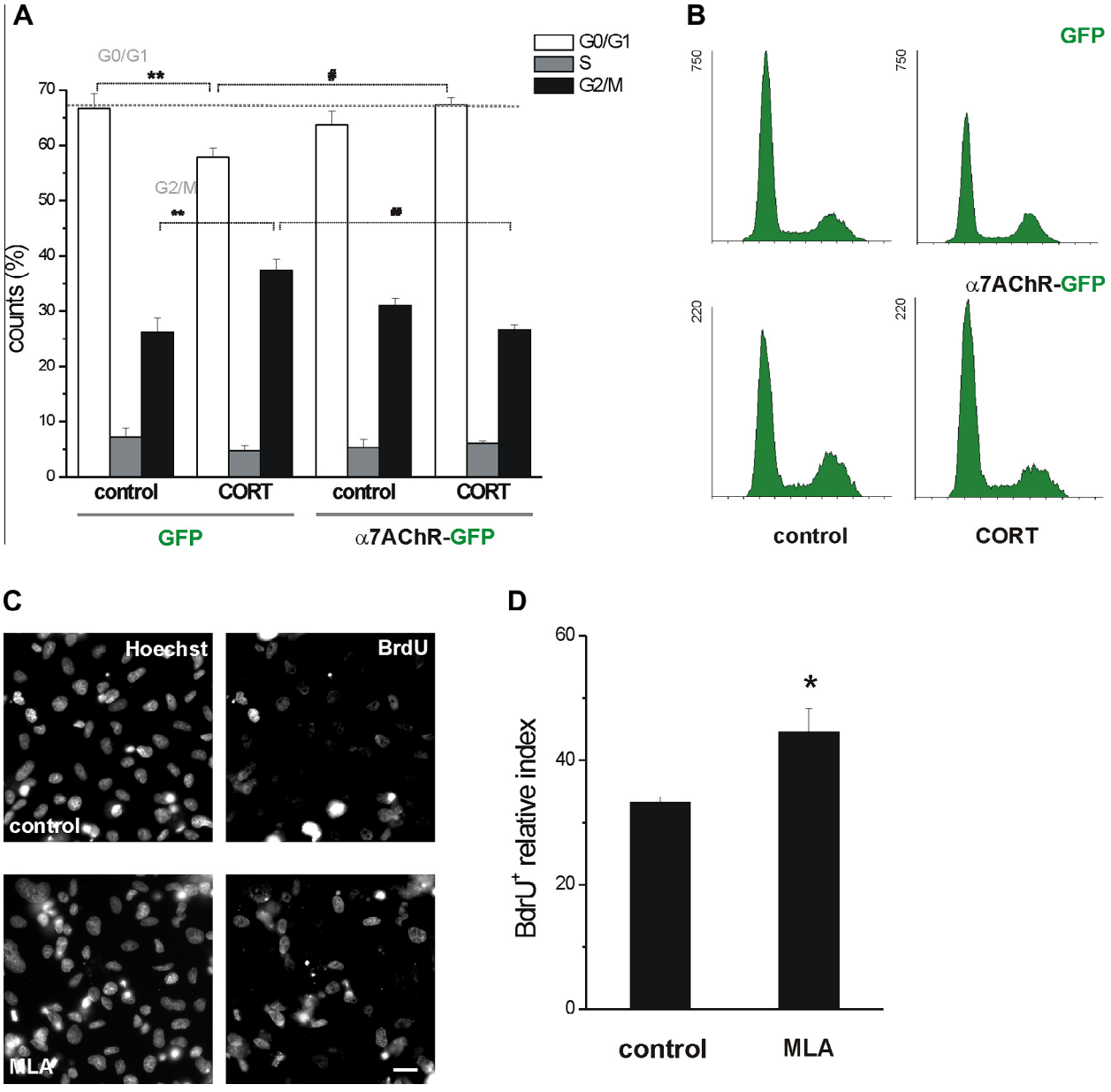

Fig. 6. Overexpression of GFP-tagged α7-AChR abolished the effects of CORT in the cell cycle. (A) CNh cells were transfected with GFP or α7AChR-GFP plasmid. Eighteen hours post transfection, cells were transferred to differentiation media and treated with 1 μM CORT or vehicle (control) for two days. Results are expressed as mean ± SEM of at least three independent experiments. Two-way ANOVA followed by simple effects was used: $p < 0.01$ for control vs. CORT factors in G0/G1 phase in GFP group; $p < 0.05$ for GFP vs. αAChR-GFP factors in G0/G1 phase in CORT group; $p < 0.01$ for control vs. CORT factors in G2/M phase in GFP group $p < 0.01$ for GFP vs. αAChR-GFP factors in G2/M phase in CORT group. (*) Denotes statistically significant differences as a consequence of CORT treatment (for each phase, respectively); (#) denotes statistically significant differences resulting from transfection. The presence of one or two symbols indicate p values < 0.05 and < 0.01, respectively. (B) Representative histograms of cell cycle of control and CORT-treated CNh cells at T2 transfected with the plasmid encoding for GFP or α7AChR-GFP. (C) Representative immunofluorescence images of CNh cells treated with 10 μM MLA (control cells were treated with the vehicle only) at T2 showing Hoechst and BrdU labeling. Scale bar = 20 μm. (D) The $BrdU^+$ proliferation index (calculated as the proportion of $BrdU^+$ cells to total cells in each field for control and MLA-treated cells at T2). Nuclei were labeled with Hoechst stain. At least 1500 cells were counted in each case. Results are expressed as mean ± SEM of four independent experiments. Student's t test, $p = 0.0292$. The presences of one symbol indicate p value < 0.05.

i.e. genomic effects. Thus, GCs may potentially have long-lasting effects on the function of various brain regions (Lupien et al., 2009). Additionally, GC could have non-genomic actions apparently mediated by binding to membrane proteins such as ligand-gated ion channels (Shi et al., 2002). The α7-AChR gene contains a cortico-steroid-response element, the genomic target of GC receptors (Leonard et al., 2002), and SP1 sites, targets for downstream signaling of glutamate receptor activation (Leonard et al., 2002; Hunter, 2012). It has been observed that GCs and chronic or prenatal stress affects α7-AChR gene expression (Carrasco-Serrano and

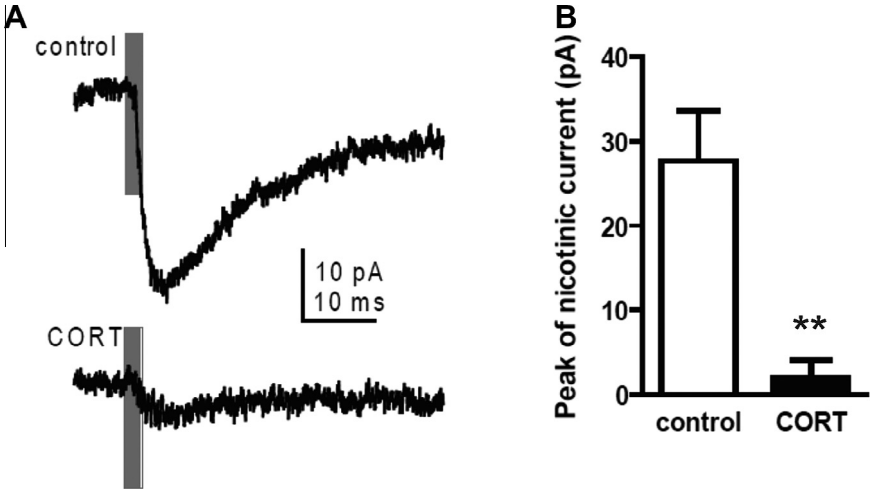

Fig. 7. CORT abolished the nicotinic response in CNh cells. (A) Example of traces depicting spikes evoked by stimulation of 50 μM nicotine in CNh cells treated with vehicle (Control) or with 1 μM CORT for two days in differentiation media. (B) Peak of nicotine currents in Control and CORT-treated CNh cells. Results are expressed as mean ± SEM of at least three independent experiments. Student's *t* test, $p = 0.0033$. (*) Denotes statistically significant differences as a consequence of CORT treatment. The presence of one, two or three symbols indicates *p* values < 0.05, < 0.01 and < 0.001, respectively.

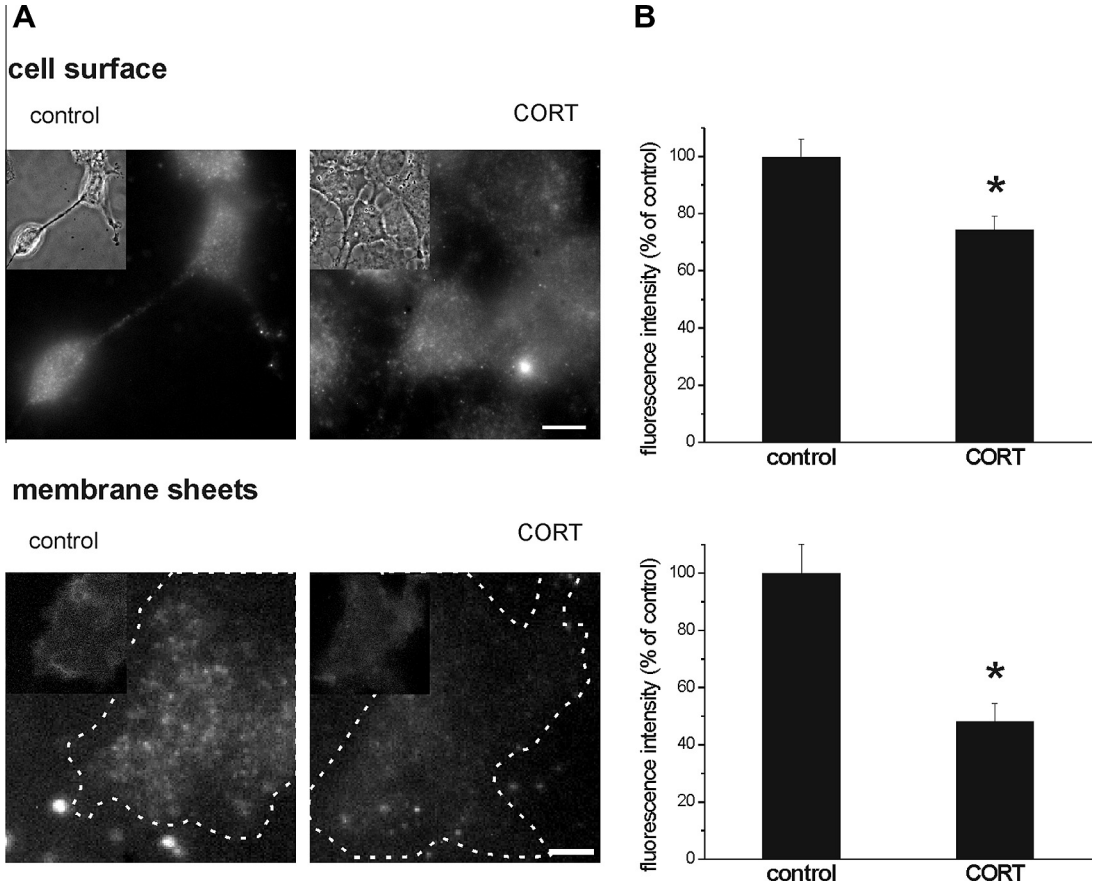

Fig. 8. CORT impaired the plasma membrane expression of α7-AChR in CNh cells. (A) Upper panel, representative fluorescence microscopy images of α7-AChR at the plasma membrane of CNh cells. Inserts in each image correspond to the respective phase contrast photograph. Scale bar = 20 μm. *Lower panel*, fluorescence microscopy images of α7-AChR at the membrane sheets from CNh cells. Insets in the images correspond to the respective TMA-DPH photographs. Scale bar = 2.5 μm. (B) Graphs representing the quantification of the corresponding images in A. Results are expressed as mean ± SEM of at least three independent experiments.

Criado, 2004; Hunter et al., 2010; Neeley et al., 2011). As a consequence of acute or chronic exposure to stress hormones, the α7-AChR could therefore be the target for genomic and non-genomic GC action. In the present work evidence that both mechanisms participate in the effects of CORT on CNh cells is presented: (1) CORT treatment significantly reduced the α7-AChR mRNA level; (2) α7-AChR levels decreased at the plasma membrane as a consequence of CORT treatment; and (3) CORT treatment practically abolished (>95%) AChR currents evoked by nicotine.

The reduction in protein expression could not account for the total loss of ionic currents observed after a nicotine pulse in CORT-treated cells. It is thus tempting to speculate that CORT exerts its action over the AChR by inhibiting its functionality as well as targeting the cell surface by both genomic and non-genomic effects.

The alteration induced by nicotine in the cell cycle demonstrated that nicotinic signaling participates in the progression of CNh cell toward a mature phenotype. Alterations induced in the cell cycle by nicotine treatment were also reported in other cell lines (Utsugisawa et al., 2002; Resende et al., 2008). It is interesting to note that nicotine treatment produced the same effect as CORT treatment, i.e. maintaining the cells in an undifferentiated state. These results could be explained in the light of evidence that chronic nicotine treatment disables AChR signaling (Ke et al., 1998) in a manner similar to that exerted by CORT. Moreover, the α7-AChR inhibitor MLA mimics the CORT action on cell proliferation in the cell model system employed in the present work. Previous work described a relationship between nicotine exposure, AChR and cyclins, key regulators of the cell cycle (Pestana et al., 2005; Chen et al., 2011). Altogether, CORT, through AChR and its downstream signaling cascade (see below), could modulate the genomic effects on the cells cycle of CNh cells.

CORT modulates adult neurogenesis in the hippocampus (Cameron and Gould, 1994) and increased levels of this GC inhibit neuronal differentiation in this cerebral area (Wong and Herbert, 2006). Chronic stress induces cycling cells in the adult hippocampus to arrest in G1 (Heine et al., 2004). In the present work CORT treatment of CNh cells was found to negatively affect arrest in the G0/G1 phase. In contrast, CORT treatment induced G0/G1 arrest in a mouse mammary hyperplastic cell line (Jiang et al., 2002). GC treatment negatively affected the proliferation of embryonic rat neural stem cells by decreasing the levels of cyclin D1 (Sundberg et al., 2006). Furthermore, dexamethasone markedly inhibited proliferation-cells entered the G0 phase-, survival and astroglial differentiation of neural stem and progenitors cells (Wagner et al., 2009).

The α7-AChR transduces the binding of acetylcholine into a rapidly desensitizing Ca^{2+} influx. This type of receptor is widely expressed throughout the mammalian brain and is involved in sensory gating, learning, memory formation and neuroprotection. Due to its high Ca^{2+} permeability it participates in various signal transduction mechanisms such as the ERK/MAPK and the JAK2/PIP3K/Akt cascades, promoting neuronal survival by inducing the production of the anti-apoptotic proteins Bcl and Bcl-x (Barrantes et al., 2010). Cells overexpressing α7-AChR have increased basal expression of Akt, which is related to cellular differentiation processes (Utsugisawa et al., 2002).

It is widely accepted that AChRs participate in neuronal development and differentiation (Hermans-Borgmeyer et al., 1989; Levey and Jacob, 1996; Svoboda et al., 2002; Falk et al., 2003; Campbell et al., 2010; Nery et al., 2010; Nordman and Kabbani, 2012; Takarada et al., 2012; Narla et al., 2013). Yet the mechanism by which synaptogenesis is coordinated during brain development remains unclear. An interesting possibility is that AChRs may play a key role in this process (Myers et al., 2005). During brain development, nicotinic responses mediate excitation and are widely distributed at early stages, largely mediated by α7-AChRs (Lozada et al., 2012). Early α7-AChR signaling is extremely important in promoting the development of glutamatergic pathways (Lozada et al., 2012). As mentioned in the Introduction, there is broad consensus that accelerated age-related cognitive decline is related to an impaired response of the HPA axis (Pardon and Rattray, 2008) and that deregulation of this axis is related to neurodegenerative conditions such as those found in Alzheimer's disease (Green et al., 2006). It has been reported that stress increases the susceptibility to develop Alzheimer's disease (Pardon and Rattray, 2008; Buynitsky and Mostofsky, 2009) and chronic stress affects gene and protein expression of α7-AChR in the rat hippocampus (Hunter et al., 2010). One could speculate that these mechanisms are operative in the developing brain of fetus exposed to GC. Based on current data, it is plausible that in the developing brain, higher CORT levels could interact with and/or modulate the expression and functionality of AChRs, finally affecting the characteristics or the fate of the affected neurons.

In conclusion, the present findings provide experimental evidence that chronic CORT treatment during cell development reduces the level of expression of AChRs and virtually suppresses nicotinic signaling in a model system. Furthermore, the data suggest a putative mechanism by which chronic stress affects an important physiological signaling pathway, ultimately impairing cell-cycle arrest and as a consequence, correct cell fate acquisition.

Acknowledgments—Thanks are due to Dr. Jon Lindstrom, Perelman School of Medicine, University of Pennsylvania, PA, for providing the mAb299 and m319 anti-AChR antibodies; to Drs. Steve Heinemann and Gustavo Dziewczapolsky, from the Salk Institute, CA, for providing the α7-AChR-GFP plasmid; to Dr. Fernanda Ceriani, Fundación Instituto Leloir, Buenos Aires, for the gift of the eGFP plasmid; to Dr. Tomás Santa Coloma, from BIOMED, Buenos Aires, for the gift of mouse anti-actin antibody and Texas Red-goat anti-mouse IgG; to Dr. A. Schinder, Fundación Instituto Leloir, Buenos Aires, and to Dr. N.P. Rotstein and L.E. Politi, Instituto de Investigaciones Bioquímicas de Bahía Blanca, Argentina, for providing the BrdU and anti-BrdU antibody; to Dr. M.I. Aveldaño, INIBIBB, Bahía Blanca, for providing the MTT; and to and to Dr. E. Pallarés, from the Faculty of Medicine, University of Buenos Aires, for her valuable help in the statistical

analysis. Research described in this article was supported by grants PICT 2008-1003 and 2011-0604 from FONCYT, Ministry of Science, Technology and Innovative Production of Argentina (MINCyT) and PIP No. 112-201101-01023 from the Scientific and Technological Research Council of Argentina (CONICET) to F.J.B and Fondecyt No 1130241 (Chile) to P.C.

REFERENCES

Allen DD, Martin J, Arriagada C, Cardenas AM, Rapoport SI, Caviedes R, Caviedes P (2000) Impaired cholinergic function in cell lines derived from the cerebral cortex of normal and trisomy 16 mice. Eur J Neurosci 12:3259–3264.

Barrantes FJ, Borroni V, Valles S (2010) Neuronal nicotinic acetylcholine receptor-cholesterol crosstalk in Alzheimer's disease. FEBS Lett 584:1856–1863.

Borroni V, Baier CJ, Lang T, Bonini I, White MM, Garbus I, Barrantes FJ (2007) Cholesterol depletion activates rapid internalization of submicron-sized acetylcholine receptor domains at the cell membrane. Mol Membr Biol 24:1–15.

Buynitsky T, Mostofsky DI (2009) Restraint stress in biobehavioral research: recent developments. Neurosci Biobehav Rev 33:1089–1098.

Cameron HA, Gould E (1994) Adult neurogenesis is regulated by adrenal steroids in the dentate gyrus. Neuroscience 61:203–209.

Campbell NR, Fernandes CC, Halff AW, Berg DK (2010) Endogenous signaling through alpha7-containing nicotinic receptors promotes maturation and integration of adult-born neurons in the hippocampus. J Neurosci 30:8734–8744.

Carrasco-Serrano C, Criado M (2004) Glucocorticoid activation of the neuronal nicotinic acetylcholine receptor alpha7 subunit gene: involvement of transcription factor Egr-1. FEBS Lett 566:247–250.

Chen CS, Lee CH, Hsieh CD, Ho CT, Pan MH, Huang CS, Tu SH, Wang YJ, Chen LC, Chang YJ, Wei PL, Yang YY, Wu CH, Ho YS (2011) Nicotine-induced human breast cancer cell proliferation attenuated by garcinol through down-regulation of the nicotinic receptor and cyclin D3 proteins. Breast Cancer Res Treat 125:73–87.

Falk L, Nordberg A, Seiger A, Kjaeldgaard A, Hellstrom-Lindahl E (2003) Higher expression of alpha7 nicotinic acetylcholine receptors in human fetal compared to adult brain. Brain Res Dev Brain Res 142:151–160.

Fukumoto K, Morita T, Mayanagi T, Tanokashira D, Yoshida T, Sakai A, Sobue K (2009) Detrimental effects of glucocorticoids on neuronal migration during brain development. Mol Psychiatry 14:1119–1131.

Gotti C, Zoli M, Clementi F (2006) Brain nicotinic acetylcholine receptors: native subtypes and their relevance. Trends Pharmacol Sci 27:482–491.

Green KN, Billings LM, Roozendaal B, McGaugh JL, LaFerla FM (2006) Glucocorticoids increase amyloid-beta and tau pathology in a mouse model of Alzheimer's disease. J Neurosci 26:9047–9056.

Heine VM, Maslam S, Joels M, Lucassen PJ (2004) Increased P27KIP1 protein expression in the dentate gyrus of chronically stressed rats indicates G1 arrest involvement. Neuroscience 129:593–601.

Hermans-Borgmeyer I, Hoffmeister S, Sawruk E, Betz H, Schmitt B, Gundelfinger ED (1989) Neuronal acetylcholine receptors in Drosophila: mature and immature transcripts of the ard gene in the developing central nervous system. Neuron 2:1147–1156.

Hunter RG (2012) Stress and the alpha7 nicotinic acetylcholine receptor. Curr Drug Targets 13:607–612.

Hunter RG, Bloss EB, McCarthy KJ, McEwen BS (2010) Regulation of the nicotinic receptor alpha7 subunit by chronic stress and corticosteroids. Brain Res 1325:141–146.

Jiang W, Zhu Z, Bhatia N, Agarwal R, Thompson HJ (2002) Mechanisms of energy restriction: effects of corticosterone on cell growth, cell cycle machinery, and apoptosis. Cancer Res 62:5280–5287.

Ke L, Eisenhour CM, Bencherif M, Lukas RJ (1998) Effects of chronic nicotine treatment on expression of diverse nicotinic acetylcholine receptor subtypes. I. Dose- and time-dependent effects of nicotine treatment. J Pharmacol Exp Ther 286:825–840.

Leonard S, Gault J, Hopkins J, Logel J, Vianzon R, Short M, Drebing C, Berger R, Venn D, Sirota P, Zerbe G, Olincy A, Ross RG, Adler LE, Freedman R (2002) Association of promoter variants in the alpha7 nicotinic acetylcholine receptor subunit gene with an inhibitory deficit found in schizophrenia. Arch Gen Psychiatry 59:1085–1096.

Lesage J, Blondeau B, Grino M, Breant B, Dupouy JP (2001) Maternal undernutrition during late gestation induces fetal overexposure to glucocorticoids and intrauterine growth retardation, and disturbs the hypothalamo-pituitary adrenal axis in the newborn rat. Endocrinology 142:1692–1702.

Levey MS, Jacob MH (1996) Changes in the regulatory effects of cell–cell interactions on neuronal AChR subunit transcript levels after synapse formation. J Neurosci 16:6878–6885.

Livak KJ, Schmittgen TD (2001) Analysis of relative gene expression data using real-time quantitative PCR and the 2(-Delta Delta C(T)) method. Methods 25:402–408.

Lozada AF, Wang X, Gounko NV, Massey KA, Duan J, Liu Z, Berg DK (2012) Glutamatergic synapse formation is promoted by alpha7-containing nicotinic acetylcholine receptors. J Neurosci 32:7651–7661.

Lupien SJ, McEwen BS, Gunnar MR, Heim C (2009) Effects of stress throughout the lifespan on the brain, behaviour and cognition. Nat Rev Neurosci 10:434–445.

Mosmann T (1983) Rapid colorimetric assay for cellular growth and survival: application to proliferation and cytotoxicity assays. J Immunol Methods 65:55–63.

Myers CP, Lewcock JW, Hanson MG, Gosgnach S, Aimone JB, Gage FH, Lee KF, Landmesser LT, Pfaff SL (2005) Cholinergic input is required during embryonic development to mediate proper assembly of spinal locomotor circuits. Neuron 46:37–49.

Narla S, Klejbor I, Birkaya B, Lee YW, Morys J, Stachowiak EK, Terranova C, Bencherif M, Stachowiak MK (2013) Alpha7 Nicotinic receptor agonist reactivates neurogenesis in adult brain. Biochem Pharmacol 86(8):1099–1104.

Neeley EW, Berger R, Koenig JI, Leonard S (2011) Strain dependent effects of prenatal stress on gene expression in the rat hippocampus. Physiol Behav 104:334–339.

Nery AA, Resende RR, Martins AH, Trujillo CA, Eterovic VA, Ulrich H (2010) Alpha 7 nicotinic acetylcholine receptor expression and activity during neuronal differentiation of PC12 pheochromocytoma cells. J Mol Neurosci 41:329–339.

Nordman JC, Kabbani N (2012) An interaction between alpha7 nicotinic receptors and a G-protein pathway complex regulates neurite growth in neural cells. J Cell Sci 125:5502–5513.

Oddo S, LaFerla FM (2006) The role of nicotinic acetylcholine receptors in Alzheimer's disease. J Physiol Paris 99:172–179.

Pardon MC, Rattray I (2008) What do we know about the long-term consequences of stress on ageing and the progression of age-related neurodegenerative disorders? Neurosci Biobehav Rev 32:1103–1120.

Pestana IA, Vazquez-Padron RI, Aitouche A, Pham SM (2005) Nicotinic and PDGF-receptor function are essential for nicotine-stimulated mitogenesis in human vascular smooth muscle cells. J Cell Biochem 96:986–995.

Resende RR, Alves AS, Britto LR, Ulrich H (2008) Role of acetylcholine receptors in proliferation and differentiation of P19 embryonal carcinoma cells. Exp Cell Res 314:1429–1443.

Schmittgen TD, Livak KJ (2008) Analyzing real-time PCR data by the comparative C(T) method. Nat Protoc 3:1101–1108.

Shi LJ, Liu LA, Cheng XH, Wang CA (2002) Modulation of neuronal nicotinic acetylcholine receptors by glucocorticoids. Acta Pharmacol Sin 23:237–242.

Sundberg M, Savola S, Hienola A, Korhonen L, Lindholm D (2006) Glucocorticoid hormones decrease proliferation of embryonic

neural stem cells through ubiquitin-mediated degradation of cyclin D1. J Neurosci 26:5402–5410.

Svoboda KR, Vijayaraghavan S, Tanguay RL (2002) Nicotinic receptors mediate changes in spinal motoneuron development and axonal pathfinding in embryonic zebrafish exposed to nicotine. J Neurosci 22:10731–10741.

Takarada T, Nakamichi N, Kitajima S, Fukumori R, Nakazato R, Le NQ, Kim YH, Fujikawa K, Kou M, Yoneda Y (2012) Promoted neuronal differentiation after activation of alpha4/beta2 nicotinic acetylcholine receptors in undifferentiated neural progenitors. PLoS One 7:e46177.

Uki M, Nabekura J, Akaike N (1999) Suppression of the nicotinic acetylcholine response in rat superior cervical ganglionic neurons by steroids. J Neurochem 72:808–814.

Utsugisawa K, Nagane Y, Obara D, Tohgi H (2002) Overexpression of alpha7 nicotinic acetylcholine receptor prevents G1-arrest and DNA fragmentation in PC12 cells after hypoxia. J Neurochem 81:497–505.

Wagner K, Couillard-Despres S, Lehner B, Brockhoff G, Rivera FJ, Blume A, Neumann I, Aigner L (2009) Prolactin induces MAPK signaling in neural progenitors without alleviating glucocorticoid-induced inhibition of in vitro neurogenesis. Cell Physiol Biochem 24:397–406.

Wang Y, Yao M, Zhou J, Zheng W, Zhou C, Dong D, Liu Y, Teng Z, Jiang Y, Wei G, Cui X (2011) The promotion of neural progenitor cells proliferation by aligned and randomly oriented collagen nanofibers through beta1 integrin/MAPK signaling pathway. Biomaterials 32:6737–6744.

Wong EY, Herbert J (2006) Raised circulating corticosterone inhibits neuronal differentiation of progenitor cells in the adult hippocampus. Neuroscience 137:83–92.

(Accepted 24 May 2014)
(Available online 4 June 2014)